Vibration signatures to identify damage in historical constructions

L. Ramos & P. Lourenço
University of Minho, Guimarães, Portugal

G. De Roeck
Catholic University of Leuven, Leuven, Belgium

A. Campos-Costa
Laboratório Nacional de Engenharia Civil, Lisbon, Portugal

ABSTRACT: The paper aims at exploring damage assessment in masonry structures at an early stage by vibration measurements. One arch replicate of historical constructions was built as reference, undamaged, state. Afterwards, progressive damage was induced and sequential modal identification analysis was performed at each damage stage, aiming to find adequate correspondence between dynamic behaviour and internal crack growth.

1 INTRODUCTION

Preservation of the architectural heritage is considered a fundamental issue in the cultural life of modern societies. Modern requirements for an intervention include reversibility, unobtrusiveness, minimum repair and respect of the original construction, as well the obvious functional and structural requirements.

In the process of preservation of ancient masonry structures, damage evaluation and monitoring procedures are particularly attractive, due to the modern context of minimum repair and observational methods, with iterative and step-by-step approaches. High-priority issues related to damage assessment and monitoring include global non-contact inspection techniques, improved sensor technology, data management, diagnostics (decision making and simulation), improved global dynamic (modal) analysis, self-diagnosing / self-healing materials, and improved predic-tion of early degradation. This paper focus on improved global (dynamic) modal analysis for damage detection.

2 DAMAGE IDENTIFICATION PROCESS

The present paper deals with the problem of damage identification by using Global and Local damage identification techniques. It is advantageous to have two categories of damage assessment methods: (a) the vibration based damage identification methods, currently defined as Global methods, because they do not give sufficiently accurate information about the extent of the damage, but they can identify its presence and define its precise location (e.g. Chang et al., 2003); and (b) the methods based on visual inspections or experimental tests, such as acoustic or ultrasonic methods, magnetic field methods, radiograph and thermal field methods (e.g. Doherty, 1987), also called as Local methods. The latter need a preceding global approach (Global methods) to detect and localize the damage, and then, if the possible location of damage is accessible in the structure, they can describe the damage in an accurate way.

Damage on masonry structures mainly relates to cracks, foundation settlements, material degradation and displacements. When cracks occur, generally they are localized, splitting the structures in macro-blocks. Dynamic based methods to assess the damage is an attractive tool to this type of structures due to the present requirements of unobtrusiveness, minimum physical intervention and respect of the original construction. The assumption that damage can be linked to a decrease of stiffness seems to be reasonable to this type of structures.

Many methods are presented in literature, see Doebling et al. (1996), for damage identification based on vibration signatures but there are only a few papers on the application to masonry structures. An important task before damage can be identified from vibration characteristics is the study and subsequent elimination of the environmental effects (Peeters, 2000), which for masonry structures can have significantly importance (Ramos, et al., 2007).

2.1 *Proposed Methodology*

Experience with other studies related to masonry structures indicates that, in several cases, simpler models (or methods) give better quality and more comprehensive results than more elaborated ones (Ramos, 2002). In this sense, it is desirable to use different techniques/tools to study the masonry structures in a holistic way. Ideally, the analyzer should have a group of methods/results to make a decision about the structure or to assist in the decision on additional studies. This is the basis for the methodology of damage identification presented next.

A group of damage methods has been selected from the literature. In one hand, it is intended to study the applicability of existing methods to the masonry structures, and, in another hand, it is aimed to have a wide view of the problem (different results are provided by different methods), assisting in the conclusions related to damage identification. If significant damage is present in the structure, the results provided from different methods would converge in a unique conclusion, giving more confidence to the analyzer.

The selected methods were applied to an arch model, where progressive and controlled damage scenarios were imposed. From the point of view of the applicability of dynamic based identification methods to masonry structures, the methodology would be successful if the detection (Level 1), the localization (Level 2) and the assessment (Level 3) will be attained with these methods. The selected methods together with the required modal information are presented in Table 1 (see Doebling et al., 1996, for the complete description of each method).

Table 1. Selected damage identification methods

Method	Expected Identification Level	Comparison to a Ref. Scenario	Modal Information				
			ω	φ	φ''	ϕ	ϕ''
Unified Significance Indicator (USI)	Level 1	Yes	•				
COMAC	Level 2	Yes		○	○	○	○
Parameter Method (PM)	Level 2	Yes	•	○	○	○	○
Mode Shape Curvature Method (MSCM)	Level 2	Yes			○		○
Damage Index Method (DIM)	Level 2	Yes			○		○
Sum of the Curvature Errors (SCE)	Level 2	Yes			○		○
Change Flexibility Method (CFM)	Level 2 and 3	Yes	•			•	○
FE Model Updating (FEMU)	Level 2 and 3	No	○	○	○	○	○

○ – Optional modal quantities; • – Compulsory modal quantities

All methods have one common aspect; they all use spatial modal information of the structure, through the mass scaled or non-scaled mode shapes ϕ and φ, respectively (or/and through the mass scaled or non-scaled curvatures mode shapes ϕ'' and φ'', respectively).

The global and local approach should be considered as complementary tasks. For the case of historical constructions these two approaches seem to be suitable, since they are non-destructive procedures to evaluate health conditions.

3 ARCH MODEL DESCRIPTION AND PRELIMINARY STUDIES

One replicate of ancient masonry arches was built with clay bricks with $100 \times 50 \times 25$ mm^3, manually produced in the Minho region, at the northern area of Portugal. The clay brick, with low compression strength, and the Mapei® mortar, with poor mechanical properties, used for the joints tries to be representative of the materials used in the historical constructions. Figure 1 shows some images of the replicate construction. The arch has a semicircular shape with a radius of 0.77 m, a span of 1.50 m, a width of 0.45 m, and a thickness of 0.05 m, and rests in two concrete abutments fixed to the ground floor with bolts.

(a) (b) (c)

Figure 1. Arch model: (a) construction initiation: (b) construction ending; and (c) arch completed

3.1 *Numerical crack prediction*

A FE model was use to predict the possible location of damage. The numerical model was built with 8 node plane stress elements in DIANA (2006). To simulate the nonlinear behavior of masonry structures the constitutive models for cracking (a combination of tension cut-off, tension softening and shear retention) was used. Nonlinearities were considered only in tensile behavior to make the analysis simpler. It should be stressed that the results are analyzed in a qualitatively way and they were useful only to predict the possible location of cracks. For that reason a sensitivity analysis was performed by changing the tensile strength of the masonry material.

Figure 2 summarizes the results of four analyses. Although the static response varies, according to the tensile strength (see Figure 2b), all the analyses shows four cracks (hinges) at ultimate load of the arch (three hinges are needed to produce a static determinate structure and four hinges are needed to form a mechanism). The numerical crack sequence is (see Figure 2a): first crack (c_1) in the intrados under the load application point; second crack (c_2) in the intrados at the right support; third crack (c_3) in the extrados and, apparently, approximately in the symmetrical position of the first crack; and the last crack (c_4) in the extrados near the left support.

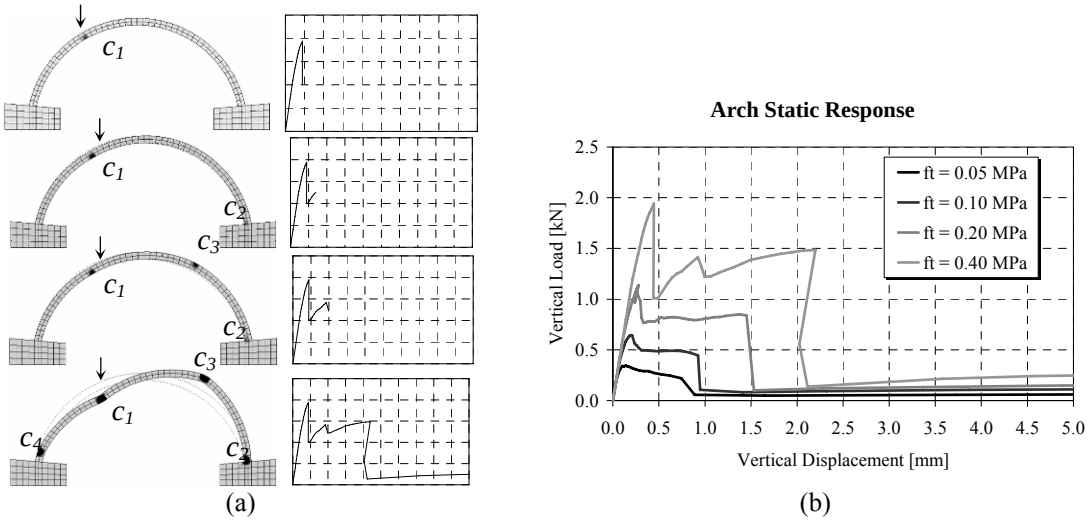

(a) (b)

Figure 2. Numerical crack prediction: (a) crack location; and (b) different static response for four values of the tensile strength f_t

3.2 *Numerical dynamic identification*

For the numerical estimation of the modal parameters a 3D finite element model with 20 noded brick elements was built in DIANA (2006) FE package. This analysis was performed to better define the experimental test planning. As the operational modal analysis was chosen for the parameter estimation (with reference and moving sensors), it is important to select the location for the reference transducers and the number of points to measure in the structure to have enough resolution of the modes shapes.

A 3D model was chosen to estimate all modes, including the out-of-plane and torsion modes. The elastic properties were the same as the previous plane stress model. Figure 3 shows the results in terms of frequency values and mode shape configurations for the first four modes. The range of frequencies starts from 36 up to 200 Hz for the first nine modes. With this analysis it was expected to have nine well spaced frequencies.

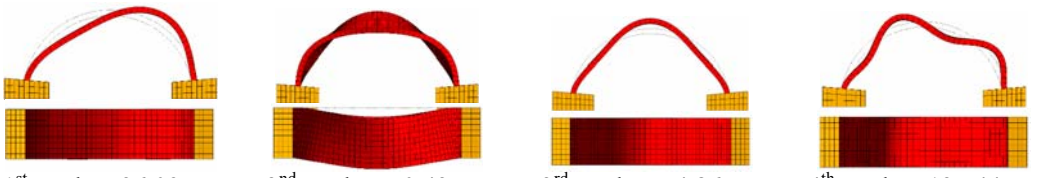

1st mode – 36.09 Hz 2nd mode – 70.43 Hz 3rd mode – 74.86 Hz 4th mode – 137.44 Hz

Figure 3. Numerical modal identification: front and top view for the first four modes

4 STATIC TESTS

Progressive and controlled damage was applied by static increasing loads to reach multiple damage levels (several cracks). The loads were applied and removed with linear branches for all the levels. Between each stage (damage scenario), modal identification analysis using output-only (ambient or natural vibration) techniques were performed, where the ambient temperature and humidity were also recorded, to evaluate possible environmental effects on the dynamic response.

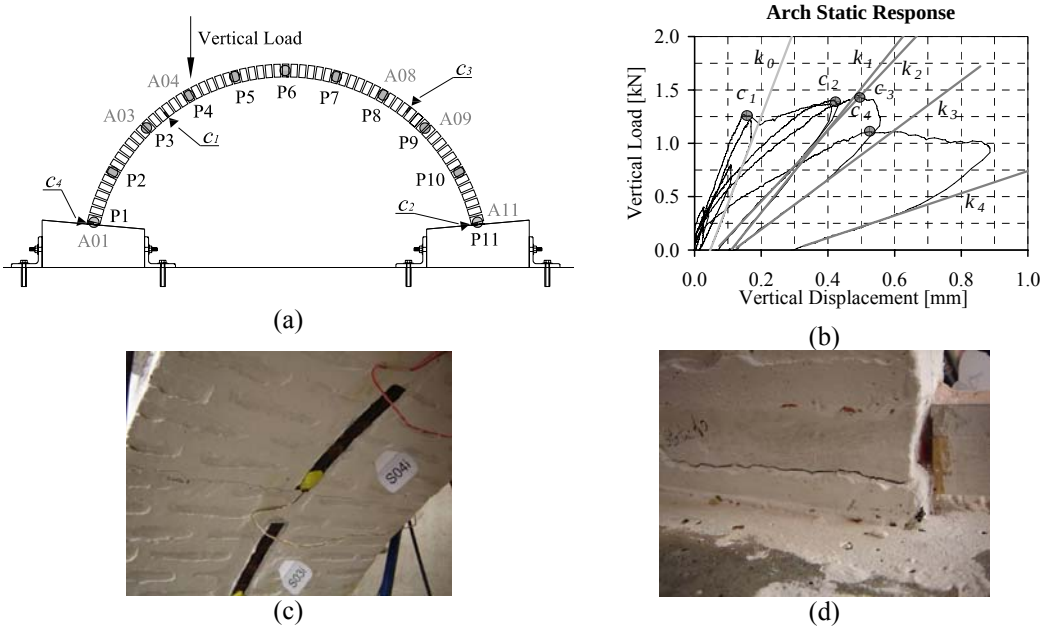

Figure 4. Static tests: (a) crack locations and sensor positions; (b) static structural response; (c) crack c_1 in the intrados; and (d) crack c_2 at the right support.

Eight Damage Scenarios (from DS_I to DS_{VIII}) were induced in the arch. The first crack (c_1) was visible in DS_V and between position P3 and P4, see Figure 4a. The others cracks appeared in subsequent scenarios, although it was not possible to make the exact correspondence between each damage level and the position of the crack. Figure 4b shows the response of the model

during the subsequent static tests, where it is possible to visualize the probable occurrence of the cracks and the stiffness decrease after each damage scenario. Figure 4c and d presents two of four cracks found in the arch. It should be stressed that the maximum remaining crack opening after the applied loads was 0.05 mm and the maximum crack depth in the loading branch was 30 mm for crack c_1 (more than half of the arch thickness).

5 DYNAMIC TESTS

Regarding the mode shapes resolution, and in order to have a clear definition of the modal displacements, it was decided to make the measurements in 11 points uniformly distributed along the arch (spaced approximately 1/8 of the arch span). This resolution is enough to have the complete definition for the first twelve modes and is feasible from the practical point of view, as too many points can be unpractical and expensive for experimental tests in real structures. The 11 points were materialized along two lines at the specimen sides for the accelerometers and along the specimen centre line for the strain gauges. In total, 44 different directions for accelerations (each side, in radial and tangential directions) and 22 strain points (intrados and extrados, in tangential direction) were measured.

Figure 5 shows some images of the sensors location in the arch. The accelerometers (A_i) were fixed to aluminum plates that were directly glued in the arch sides, in order to measure in the normal and tangential directions. The size of the strain gauges (S_i) is shown in detail in Figure 4c. The length of 12 cm is justified for having representative information of the homogenous masonry behavior, as the strain gauge crosses three bricks.

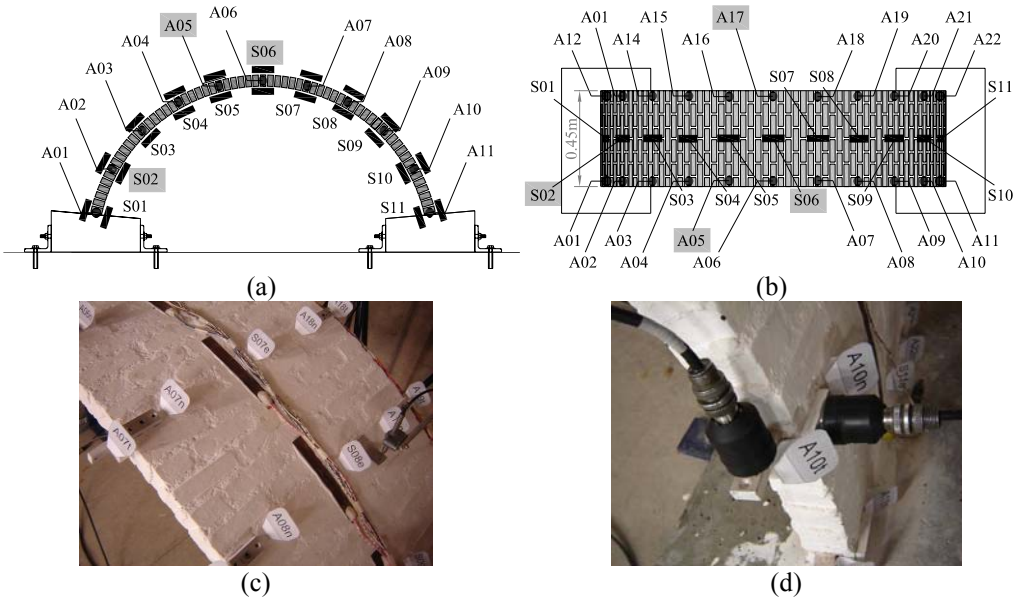

Figure 5. Location of the measuring points for the dynamic tests: (a) front view; (b) top view; (c) one test setup; and (d) normal and tangential accelerations measurements.

The dynamic tests were performed under two different type of excitations: ambient and random impacts introduced by an impact hammer. Only with random impact excitation was possible to measure with accuracy the modal strains in the arch.

6 DAMAGE ANALYSIS

Before any attempt to estimate the damage directly from experimental results, a series of numerical crack simulations were performed with the aim to study the applicability of the selected damage methods. The analysis accomplished the construction of three different FE models and the cracks were simulated by three different procedures. After this study, the damage methods were applied to the experimental modal data.

6.1 *Numerical damage simulation*

In the first model, model A, see Figure 6a, the crack was idealized by means of a localized crack with spring elements in a line between two opposite measuring points, at the front and back edges of the arch. In the second model, model B, the crack was localized between two pairs of opposite measuring points, see Figure 6b, and again with spring elements. In the last model, model C, the crack was simulated by means of the reduction of the Young's modulus in a band of elements with 0.10 m length, see Figure 6c.

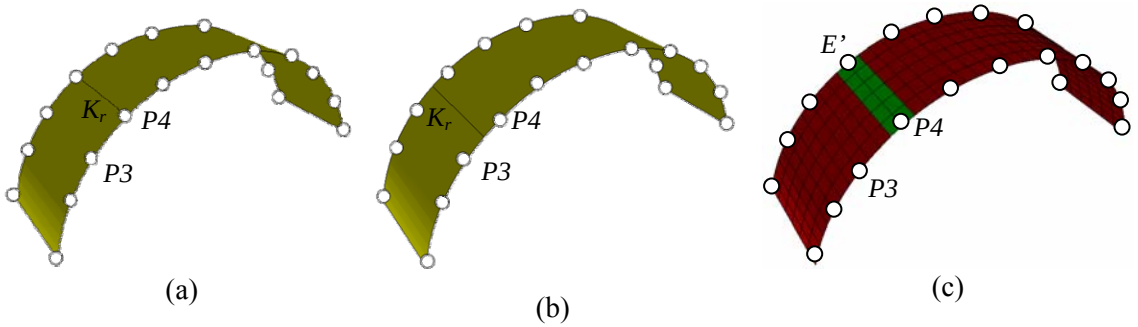

Figure 6. Numerical models: (a) model A; (c) model B; and (c) model C

In model A and C the crack location was at position P4 (see Figure 6a and Figure 6c) and in model B between the positions P3 and P4 (in the real position of crack c_1 of the experimental tests). The aim of the two different locations was to study if damage methods could locate the vicinity of the damage, even if the measurements were not in the exact position of the damage.

On each model, three different Damage Scenarios (DS_I, DS_{II}, and DS_{III}) were simulated by three different crack depths of 7.5, 15 and 30 mm, which corresponds to a cross section reductions of 15, 30 and 60% (the arch thickness is equal to 50 mm), respectively. The spring stiffness K_r of the models A and B was calculated by the method based on the facture mechanics theory, presented by Chondros et al (1998). As an example of the numerical crack simulation, Figure 7 presents the results for the case of model A with a crack of 15 mm depth (DS_{II}), see Table 1 for the notation of the methods used. Information for the other models and different damage scenarios will be provided in another publication.

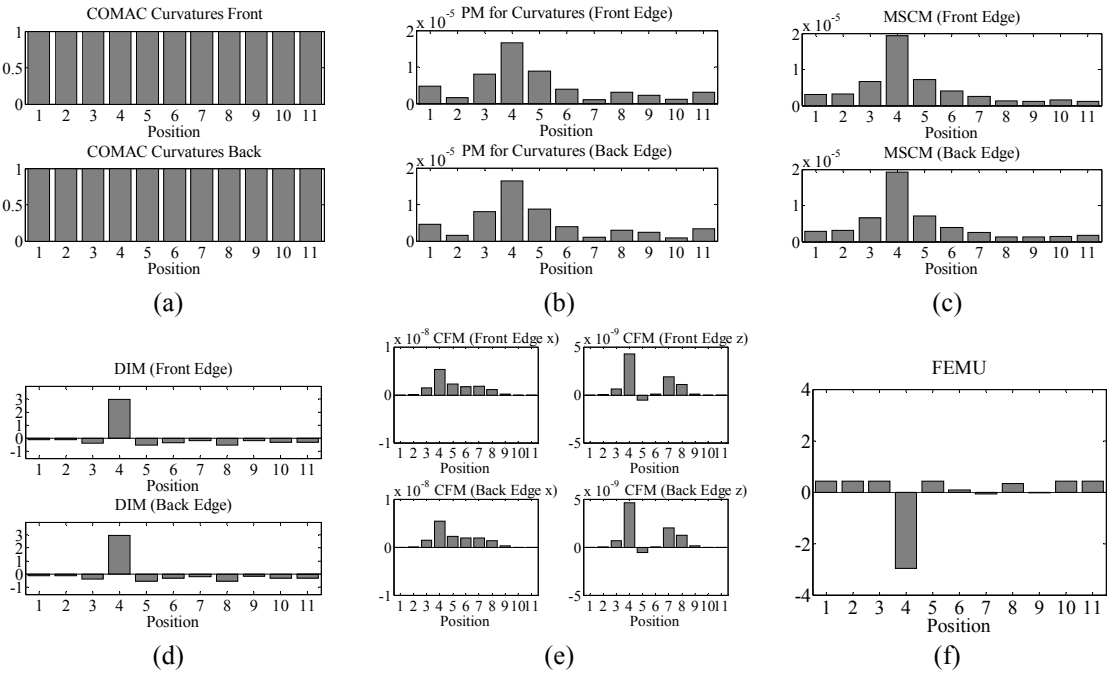

Figure 7. Damage analysis of model A for the 15 mm crack depth scenario (DS_{II}): (a) COMAC; (b) PM; (c) MSCM; (d) DIM; (e) CFM; and (f) FEMU

The damage in this model was simulated at position P4. The methods with direct modal information were applied separately in both arch edges; front and back. As similar with the others cases, the COMAC values were insensitive to the presence of damage (see Figure 7a), but the others methods shown that it is possible to locate the damage at position 4 by mode shape changes and/or curvature mode shape changes. The DIM and FEMU methods, see Figure 7d and Figure 7f, seem the most capable to localize (Level 2) and to quantify (Level 3) damage.

6.2 *Experimental Global Parameters*

Table 2 presents the frequency results for the progressive damage scenarios and Figure 8a gives the relative variation of the frequencies. Observing the global frequency results, the modal properties of the masonry specimens seem sensitive to the damage progress. The residual values in the last scenario are between 78 and 95% of the reference values. These results seem promising, as other tests in the literature report smaller changes in frequencies values, see Doebling, et al. (1996). A significant increase of damping was observed after DS_{IV}, see Figure 8b, where the average values for the damping coefficients using 6 and 7 mode shapes are presented.

Table 2. Frequency results for the arch model with ambient excitation

Damage Scenario	Mode 1			Mode 2			Mode 3			Mode 4		
	ω [Hz]	CV [%]	Δω [Hz]	ω [Hz]	CV [%]	Δω [Hz]	ω [Hz]	CV [%]	Δω [Hz]	ω [Hz]	CV [%]	Δω [Hz]
RS	35.59	0.57	–	67.30	0.69	–	72.11	0.53	–	125.74	0.52	–
DS_I	35.55	0.44	–0.05	67.51	0.61	+0.21	71.80	0.27	–0.30	125.69	0.76	–0.05
DS_{II}	35.55	0.34	–0.04	67.39	0.83	+0.09	71.83	0.74	–0.28	125.79	0.81	+0.05
DS_{III}	35.42	0.44	–0.17	67.47	0.88	+0.17	71.66	0.66	–0.45	125.75	0.88	+0.01
DS_{IV}	35.15	0.34	–0.44	67.11	0.66	–0.19	71.33	0.41	–0.78	126.01	0.43	+0.28
DS_V	33.72	0.48	–1.87	65.68	0.54	–1.62	69.36	0.43	–2.75	124.48	0.64	–1.25
DS_{VI}	33.19	0.52	–2.40	64.91	0.79	–2.39	68.56	0.42	–3.55	123.58	0.56	–2.16
DS_{VII}	31.49	0.69	–4.10	63.08	1.02	–4.22	65.72	0.52	–6.39	121.97	0.75	–3.77
DS_{VIII}	28.09	1.11	–7.50	58.44	1.20	–8.86	62.61	0.74	–9.50	119.44	0.74	–6.30

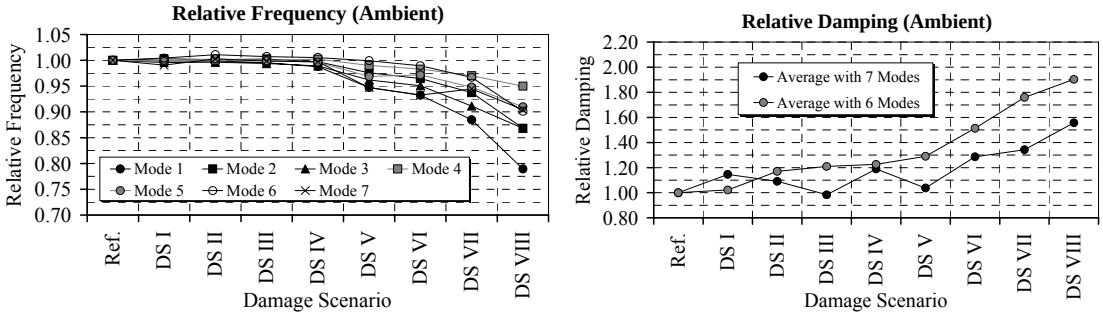

(a) (b)

Figure 8. Dynamic global response: (a) relative frequency variation; and (b) relative damping variation.

6.3 *Experimental damage analysis with non-model based methods*

Starting with the results form the USI method (see notation in Table 1), Figure 9 shows for both types of excitation the results for the comparisons with the Reference Scenario (RS) and the relative comparisons for each consecutive DS. In this analysis all the 7 estimated frequencies were considered. One conclusion emerged is the different values order before and after DS_V, appointing that some significant change happened in this scenario. The following value, DS_{VI}, is about the same order and in the last two a significant increasing is observed. These results indicate that when the USI is calculated for the several scenarios the detection of damage (Level 1) is possible and it confirms the analysis of the global parameters. For the case of no

information about the modal information history, the detection of damage with USI might be difficult to predict, because no reference values in the undamaged condition are compared.

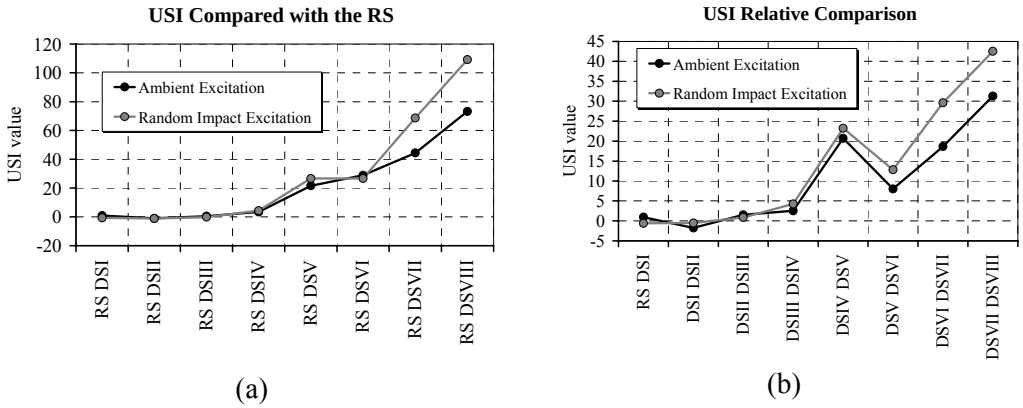

Figure 9. USI results: (a) Compared with the RS; and (b) relative comparison

Concerning the others non-model based methods (COMAC, PM, MSCM, DIM, SCE and FCM) some assumptions were made to increase the results quality. On each curvature mode shape the values close to zero were neglected in order to avoid any contamination in the results. Also, not all the modes were considered. As the 7th mode shape components were not well estimated, only the first six modes were considered. In this way, only the significant values for curvatures and well estimated modes were compared, which makes the analysis more reliable.

With the non-model based methods three different comparisons were performed: (a) the comparison of each DS to the RS; (b) the comparison for each consecutive DS; and (c) the comparison of each DS to the DS_{III}. For all the analyses the experimental modal curvatures were used and, in general, the following conclusions were taken:

- The COMAC values calculated for both modal displacements and the modal curvatures are inconclusive or they are insensitive to the damage location, in accordance with the numerical crack simulation presented in Section 6.1;
- The PM only gave the precise location for the case of the comparison with the RS until the DSIV and for some cases of consecutive comparisons, with better performance for the results with modal displacements;
- The MSCM, the DIM and the SCE gave similar results and they were able to locate the damage in the vicinity of the experimental crack locations;
- The majority of the results from CFM were inconclusive. Only for the lasts DS the results with modal curvatures are coincident the MSCM. This observation might be related to the fact that the modes used in this analysis were scaled to the mass matrix with the scale factors obtained experimentally in the preliminary tests at RS. However, scale factors calculated during each DS in the numerical crack simulation shows significant differences between each scenario. As the CFM requires scaled modes, the results can be contaminated with noise introduced by the adopted scale factors from the RS.

As an illustration of the preceding conclusions, Figure 10 presents the results for the relative comparison between the DS_{IV} and DS_V, where is clear an evidence of a damage at positions P1 and P11 for the MSCM and FCM for modal curvatures and a damage at position P1 and P7 for the DIM and SCE.

Considering the above conclusions, the seeking of the damage location was based in the analysis of the results from the methods which gave consistence results, namely the MSCM, the DIM and the SCE. Figure 11 present the final location results for the three different comparisons.

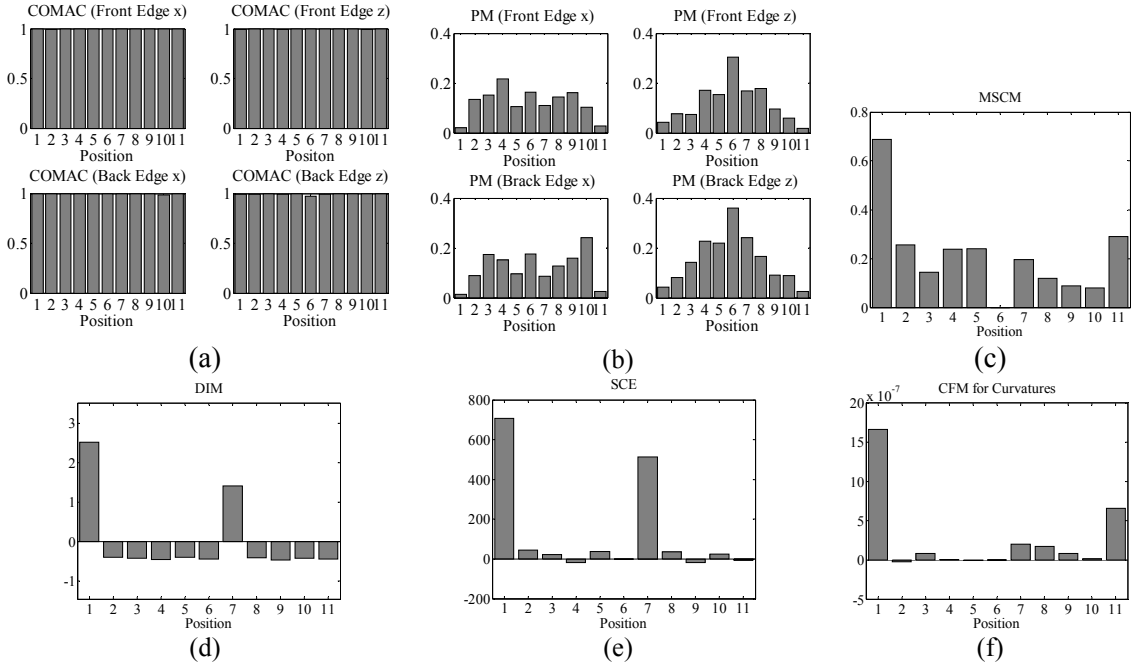

Figure 10. Results with measure curvatures for the comparison between DS_{IV} and DS_{V}: (a) COMAC; (b) PM; (c) MSCM; (d) DIM; (e) SCE; and (d) CFM for curvatures;

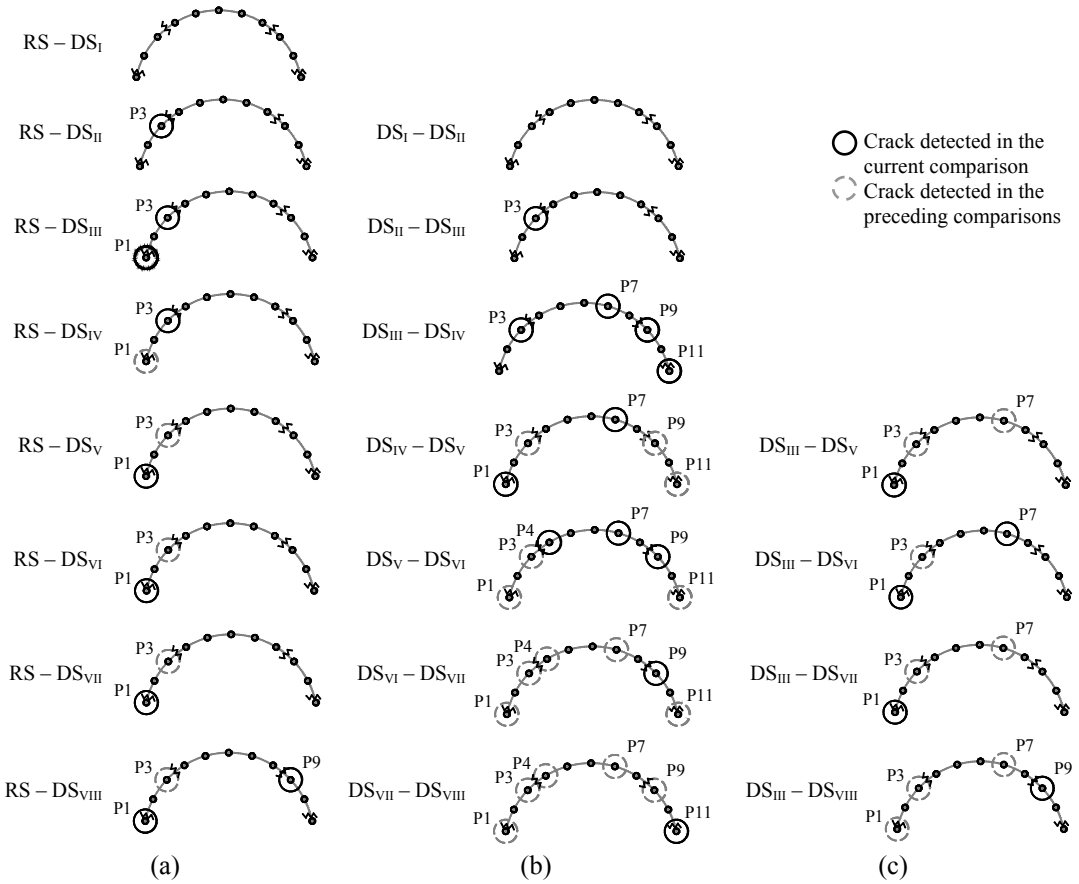

Figure 11. Damage location: (a) comparison with the RS; (b) consecutive comparison with each DS; and (c) comparison with DS_{III}

From Figure 11 it was possible to conclude the following:

- The analysis based with the RS (see Figure 11b), shows the first crack c_1 (see Section 4) even before the notorious occurrence on DS_V. Only three cracks were located at positions P1, P3 and P9 in this analysis.
- For the case of consecutive comparisons (see Figure 11b), all the cracks were located in the vicinity of the observed experimental positions, namely P1, P3/P4, P7/P9 and P11.
- In the last analysis, the comparison with DS_{III} (see Figure 11c), only three cracks were located in the same position as the analysis with the RS (P1, P3 and P7/P9).

Considering the above results, it seems that the combination of several damage methods based on experimental modal curvatures is a good methodology to detect and locate accurately and at an earlier stage the damage in the case of the masonry arch.

7 CONCLUSIONS

This paper presents a damage analysis of an arch model studied in the laboratory. Controlled damage scenarios were applied and a damage analysis was performed with a selected group of methods by means of vibration signatures. The group of damage methods have a common feature: they all use spatial modal information, especially the modal curvatures, for damage identification.

The global results from the damage scenarios reveal that the modal properties of the masonry specimen are sensitive to the induced damage. In terms of frequency results, the frequency values significantly decrease at progressing damage, more then reported for other structures in the literature.

The selected group of damage methods demonstrate that damage can be successfully localized based on dynamic changes, especially if model curvatures are taking in to account. The cracks at an earlier stage were localised in the arch model.

The application of finite element model updating techniques is still in progress. Difficulties were founded to tune experimental data of each damage scenario with the same numerical model. One of the conclusions emerged from the numerical crack simulation was the high sensitivity of the arch dynamic response to the arch geometry. Hence during the several damage scenarios it was observed residuals deformations on each static test, for each scenario it seems to be necessary to tune also the geometry of the numerical model, together with rotational stiffness for crack simulation.

If these observations are confirmed with real case studies, such as buildings, bridges or towers, the vibration based damage identification techniques applied to similar masonry constructions can be a useful tool in the conservation process of ancient masonry structures.

REFERENCES

Chang, P.C.; Flatau, A.; Liu, S.C. 2003. Review Paper: Health Monitoring of Civil Infrastructure, Structural Health Monitoring, Vol. 2 (3), pp. 257-267

Chondros, T.G.; Dimarogonas, A.D. and Yao, J. 1998. A Continuous Cracked Beam Vibration Theory, Journal of Sound and Vibration, 215(1), pp. 17-34

DIANA User's Manual 2006. Release 9, TNO DIANA, the Netherlands

Doebling, S.W.; Farrar, C.R.; Prime, M.B.; Shevitz, D. 1996. Damage identification and health monitoring of structural and mechanical systems from changes in their vibration characteristics: a literature review, Los Alamos National Laboratory, NM

Doherty, J.E. 1987. Non-destructive Evaluation, Handbook on Experimental Mechanics, A.S. Kobavashi Edt., Society for Experimental Mechanics, Chapter 12

Peeters, B. 2000. System Identification and Damage Detection in Civil Engineering, PhD Thesis, Catholic University of Leuven, Belgium

Ramos, L.F. 2002. Experimental and Numerical Analysis of historical Constructions (in Portuguese), Master Thesis in Civil Engineering, University of Minho, www.civil.uminho.pt/masonry, 400 p.

Ramos, L.F.; Marques, L.; Lourenço, P.B.; Roeck, G., Campos-Costa, A.; Roque, J. 2007. Monitoring Historical Masonry Structures with Operational Modal Analysis: Two Case Studies, 2nd International Operational Modal Analysis Conference, Copenhagen, April 30–May 2, 2007, vol. 1, pp. 161-168